Intrinsic Dispersivity of Randomly Packed Monodisperse Spheres

U. M. Scheven*
REQUIMTE/CQFB, Departamento de Química, FCT-Universidade Nova de Lisboa, 2829-516 Caparica, Portugal

R. Harris and M. L. Johns
Magnetic Resonance Research Laboratory, Department of Chemical Engineering, University of Cambridge, Cambridge CB2 3RA, United Kingdom

(Received 7 May 2007; published 1 August 2007)

We determine the intrinsic longitudinal dispersivity l_d of randomly packed monodisperse spheres by separating the intrinsic stochastic dispersivity l_d from dispersion by unavoidable sample dependent flow heterogeneities. The measured l_d, scaled by the hydrodynamic radius r_h, coincide with theoretical predictions [Saffman, J. Fluid Mech. **7**, 194 (1960)] for dispersion in an isotropic random network of identical capillaries of length l and radius a, for $l/a = 3.82$, and with rescaled simulation results [Maier *et al.*, Phys. Fluids **12**, 2065 (2000)].

DOI: 10.1103/PhysRevLett.99.054502 PACS numbers: 47.56.+r

Tracer dispersion in noninertial flow through random porous media is of considerable importance in catalysis, chromatography, ground water flows, oil production, and soil contamination, and it is a fundamental problem of hydrodynamics. Absent macroscopic stagnation zones, it is governed by differential advection in a nonuniform velocity field coupled to diffusion along velocity gradients perpendicular to the local flow. In laminar flow through a pipe [1–3] the pipe radius a sets the spatial scale for the velocity gradients. In a simple isotropic random porous medium, realized approximately in the laboratory with a random pack of identical spheres (RP), the equivalent length is given by the volume to surface ratio of the pore space, defining the hydrodynamic radius $r_h = V/S$. Additionally, a second length l sets the scale for ''mechanical mixing'' of the flow by geometric randomness of the pore space. The random network of identical capillaries has the required two lengths l and a, the length and radius of a capillary, respectively, and is therefore the simplest spatially random model which could reasonably be expected to have the dispersive properties of a jammed random pack of spheres [4,5]. We show this to be the case.

The proper description of dispersion in packed beds of monodisperse spheres has remained an open question because published experimental results are scattered, not untypically by factors two to five, and ranging up to a decade [6,7]. This is so, first, because variations of order and porosity in the packed bed affect dispersion differently from one sample to the next. The spatial arrangement of a RP belongs to a set of configuration states with porosities ε anywhere between $0.26 < \varepsilon < 0.48$ and with varying degrees of local and global order. $\varepsilon = 0.26$ corresponds to fcc packing, while the maximally random jammed state has a porosity of $\varepsilon \approx 0.37$ [8]. No RP is maximally random because ordered domains with increased porosity are always present near the walls of the container [9], and because localized crystalline domains can and do occur, depending on the packing protocol [10,11]. Second, the flow entry may be nonuniform despite the use of flow distributors. The inhomogeneity of the injected flow tends to be unknown or unquantified in all experiments, including our own. Consequently, all published measurements of dispersion in ''random packs'' of spheres should be regarded as upper bounds on the intrinsic value. We use displacement encoding pulsed field gradient nuclear magnetic resonance to measure tracer dispersion as a function of displacement in noticeably different packs. In the data analysis we separate intrinsic stochastic dispersion from that caused by the unavoidable macroscopic flow heterogeneities caused by faster flow near the wall or by imperfect flow injection.

Four packs were made from the constituent spherical glass particles with a polydispersivity of approximately 5%; for three packs ($P1$, $P2$, $P3$) the particle mean diameter was $d = 100$ μm, and for the fourth ($P4$) it was $d = 500$ μm. The particles were filled, under water, into a cylindrical vessel of diameter 37.5 mm and length 70 mm and closed with inlet and outlet end caps containing flow distributors. The sealed package was then connected to twin piston pumps via semirigid tubing, and placed into the magnet and imaging gradient set of an 85 MHz Bruker NMR system. By imaging the samples we verified complete filling of the void space with water. The piston pumps were turned on to deliver constant and controlled volumetric flow at Péclet numbers $10 < \mathrm{Pe} = v_0\lambda/D_m < 450$, with $\lambda = 6r_h$, the mean flow velocity v_0, and the diffusion coefficient of water $D_m = 2.1$ μm^2/ms. Displacement encoding NMR experiments were performed, for different evolution times Δ corresponding to different mean displacements $\zeta_0 = v_0\Delta$. We used the 13-interval sequence pulsed field gradient sequence described by Cotts [12], which produces a signal $S(q) = \langle e^{iq\zeta_j}\rangle$, where q is the magnitude of the magnetization wave vector $\vec{q}$ set up by the pulsed field gradients and ζ_j is the displacement of spin

j during Δ, all parallel to the direction of mean flow. This signal is equal to the qth Fourier component of the probability distribution of molecular displacements $P(\zeta)$. A cumulant [13,14] analysis of $S(q)$ sampled at low q yields the variance σ^2 and skewness γ^3—the second and third central moments, respectively—of $P(\zeta)$, with error bars [15]. The porosities of all samples were determined from $\varepsilon = \dot{V}/A v_0$ where $\dot{V}$ is a volumetric flow rate, v_0 is the corresponding measured mean flow velocity, and A is the cross section of the tube. Measured porosities for ($P1$, $P2$, $P3$, $P4$) are $\varepsilon = (0.352, 0.367, 0.374, 0.341)$ and are known to better than 1% of the stated value.

The spatial and temporal evolution of displacement distributions can be mapped using the cumulant derived skewness factor γ^3/σ^3, shown in Fig. 1 for packs $P1$, $P3$, and $P4$. There are three stages to the evolution of the displacement distribution. For short mean displacements (I) of less than approximately 0.8 bead diameters the displacement distribution reflects the velocity distribution within a pore [16], smeared by diffusion across stream lines. For intermediate mean displacements (II) the skewness drops, approximately logarithmically, with mean displacement. The coincidence of the data with Pe = 88 and Pe = 440 indicates that beyond Pe = 88 this is a mechanical effect scaling with sphere size. Linear extrapolation of the drop in skewness suggests that a normal asymptotic distribution with zero skewness might appear for mean displacements beyond eight or ten bead diameters, but for the largest mean displacements (III) the skewness remains finite, small, and approximately constant. This persistent deviation from normality signals the presence of macroscopic flow heterogeneities, and in the following sections we shall analyze data acquired in this "quasiasymptotic" regime (III).

We first consider a subensemble $\mathcal{E}_i$ of tracers starting out in the same pore labeled by index i at time $t = 0$. At $t = \Delta$ these have swept through a domain of the sample whose length is approximately $\langle\zeta\rangle_i$, thus defining a drift velocity associated with the pore of origin $v_i = \langle\zeta\rangle_i/\Delta$. Lateral

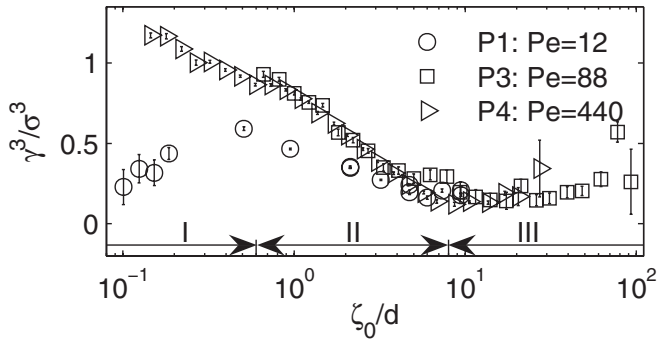

FIG. 1. Skewness factor γ^3/σ^3 of the displacement distribution $P(\zeta)$, as a function of scaled mean displacement ζ_0/d. σ^2 and γ^3 are the variance and skewness of $P(\zeta)$: (I) velocity distribution smeared by diffusion; (II) transition regime; (III) quasiasymptotic regime.

dispersion of tracers in $\mathcal{E}_i$ occurs approximately by a random walk producing a Gaussian transverse displacement distribution of width $l_t = \sqrt{2k_t\langle\zeta\rangle}$, where $k_t \approx r^2/d = d/4$ is the approximate and purely geometric transverse dispersivity, taking the scattering length to be the sphere radius r and the spatial scattering frequency to be d^{-1}. The volume swept by tracers in $\mathcal{E}_i$ defines the approximate spatial coarse graining volume of the NMR displacement encoding measurement. For our experiments in the column of diameter $D = 37.5$ mm the estimated RMS lateral dispersion is less than $D/20$ for pack $P4$ and less than $D/50$ for packs $P1$, $P2$, $P3$, implying poor transverse mixing over the experimental time scales. The drift velocities v_i associated with different pores i in the sample deviate from the mean velocity v_0 by $\delta v_i \equiv v_i - v_0$. Dropping the subscript, we describe δv by a normalized distribution $P_v(\beta)$, $\beta = \delta v/v_0$, and $\langle\beta\rangle = 0$. We assert the effective absence of stagnant or recirculation zones $P_v(\beta \le -1) = 0$, where effective means that experimental times are long enough to allow tracers located near walls to diffuse into the flow. Then, for creeping flows the distribution $P_v(\beta)$ depends on the homogeneity of flow injection, the homogeneity of the pore space, and on the size of the experimental coarse graining volume. If $P_v(\beta)$ varies on transverse and longitudinal length scales larger than those of the experimental coarse graining volume, then $P_v(\beta)$ is a stationary distribution, for the purposes of our data analysis. We do not know the shape of $P_v(\beta)$, but denote its variance and skewness by $\langle\beta^2\rangle$ and $\langle\beta^3\rangle$, respectively. Finally, we recall that the Carman-Kozeny [17] expression for the permeability of a packed bed scales as $K \propto \varepsilon^3/(1-\varepsilon)^2$, while the dispersivity of a packed bed is much less sensitive to porosity, scaling with the average interparticle distance as $\varepsilon^{1/3}$. In our data analysis we therefore allow for velocity variation within the sample, caused by small variations of the local porosity, but assume a uniform dispersivity l_d.

Suppose now that $P_v(\beta)$ is stationary, describing, for example, fast flow in a thin annulus along the entire wall of the tube as well as large scale heterogeneities caused by uneven flow injection. Then, in the quasiasymptotic limit $\zeta_0 = Nd$, $N \gg 1$ and in a frame comoving with the mean flow at velocity v_0 we can write the central moments $\langle\xi^n\rangle$, $\xi = \zeta - \zeta_0$, of the tracer displacement distribution as a convolution of a dispersive Gaussian displacement distribution with a distribution of mean displacements governed by $P_v(\beta)$,

$$\langle\xi^n\rangle = \frac{1}{\sqrt{2\pi}} \iint P_v(\beta) \frac{\xi^n}{\sigma_\beta} e^{-(\xi-\beta\zeta_0)^2/2\sigma_\beta^2} d\xi d\beta, \qquad (1)$$

where $\sigma_\beta^2 = 2l_d(1+\beta)\zeta_0$ is the variance of displacements for tracers originating in a pore associated with drift velocity $v_0(1+\beta)$. Then the variance and skewness of the tracer displacement distribution integrate to $\sigma^2 = 2l_d\zeta_0 + \langle\beta^2\rangle\zeta_0^2$ and $\gamma^3 = 6l_d\zeta_0^2\langle\beta^2\rangle + \langle\beta^3\rangle\zeta_0^3$, respectively. Thus, for large displacements ζ_0, the measured skewness factor

γ^3/σ^3 tends toward the skewness factor of $P_v(\beta)$ given by $\langle\beta^3\rangle/\langle\beta^2\rangle^{3/2}$. The observed finite, positive, and approximately constant skewness factor in the quasiasymptotic regime (III) of Fig. 1 is therefore consistent with our supposition of a stationary $P_v(\zeta)$. Furthermore, the positive and finite skewness is consistent with the presence of a thin annulus of faster flow near the tube walls. Dividing the expression of σ^2 by $2\zeta_0$, we obtain a function for what is commonly termed the effective dispersivity

$$\sigma^2/2\zeta_0 = l_d(\mathrm{Pe}) + \frac{1}{2}\langle\beta^2\rangle\zeta_0, \tag{2}$$

which clearly separates an intrinsic dispersivity $l_d(\mathrm{Pe})$ from the sample dependent spreading of tracers caused by finite $\langle\beta^2\rangle$. For later reference, this implies that tracer elution measurements with packs of length L measure a constant excess dispersivity of $\frac{1}{2}L\langle\beta^2\rangle_L$, and similarly NMR experiments conducted at fixed mean displacements $\zeta_0 \ll L$ measure a constant excess dispersivity of $\frac{1}{2}\zeta_0\langle\beta^2\rangle_{\zeta_0}$. Figure 2 plots the effective dispersivity as a function of mean displacement, scaled to the particle diameter, for three flow experiments through pack $P3$. In the quasiasymptotic regime (III) data are plotted with solid symbols, and here the behavior is approximately linear indeed. The solid lines are obtained by fitting the entire data set to three values of $l_d(\mathrm{Pe})$ and a common slope $\frac{1}{2}\times\langle\beta^2\rangle$. The intersections of fits with the y axis measure the intrinsic Péclet-number dependent dispersivity of the unconfined pack. The equivalent plots for samples $P1$-$P4$ look similar, with respective values of $\langle\beta^2\rangle^{1/2} = (0.037, 0.066, 0.056, 0.06)$, and are not shown here. Incidentally, a similar approximately linear dependence of "effective" dispersivity on mean displacement clearly appears in simulations [18] of flow through a tube of diameter D packed with spheres of diameter $d = D/48$, for which $\langle\beta^2\rangle^{1/2} \approx 7.7\%$.

Now we compare intrinsic dispersivities $l_d(\mathrm{Pe})$ measured in the four bead packs with each other, with Maier's simulations [19] and with Saffman's theory [5]. In order to map all results onto each other we need to scale the experimental, numerical, and theoretical dispersivities by a reference length characterizing each pore space. Scaled by sphere radius and shown in Fig. 3(a), the experimental and simulated results do not fall onto a universal curve. However, they do when scaled by the hydrodynamic length $\lambda = 6r_h$, and this is shown in Fig. 3(b). r_h is the hydrodynamic radius which also governs the permeability of packed beds [7,17], and the conventional factor 6 is chosen for ease of comparison with published dispersion coefficients $D_\parallel = l_d v_0 = l_d \mathrm{Pe} D_m/\lambda$. For packed spheres $\lambda_s = d\varepsilon/(1-\varepsilon)$, where d is the sphere diameter. For simulated packed spheres represented with orthogonal surfaces on a Cartesian grid $\lambda_{\mathrm{sim}} = \frac{2}{3}\lambda_s$; the factor $2/3$ enters because the surface area A of the gridded sphere is $A = 6\pi r^2$. Finally, for capillaries of radius a the hydrodynamic length $\lambda_c = 3a$. The experimental data in Fig. 3(b) fall, approximately, onto a straight line which is fitted by $l_d/\lambda \approx [A\ln(\mathrm{Pe}) + B]$, with $A = 0.120 \pm 0.007$ and $B = 0.11 \pm 0.03$, and $\mathrm{Pe} = v_0\lambda/D_m$. The systematic agreement between samples having different porosities and the near coincidence of the fit to the data with Maier's simulation results confirms both the scaling of the dispersivity with λ and the need to count the true surface of the numerical spheres. To compare with theory we rewrite Saffman's result for the dispersion coefficient of the capillary network as its dispersivity scaled by λ_c.

$$l_d/\lambda_c = \theta/18 \times [\ln(\theta/2) + \ln(\mathrm{Pe}) - 17/12] - \mathrm{Pe}/432 + 7/9/\mathrm{Pe} + \mathcal{O}(1/\mathrm{Pe}^2). \tag{3}$$

Plotted in Fig. 3(b) with a thick dashed line ($\theta = 3.82$) this expression coincides with the linear fit to our data, for the range of $\mathrm{Pe} \ll 24\theta$ where expression (3) is valid. This

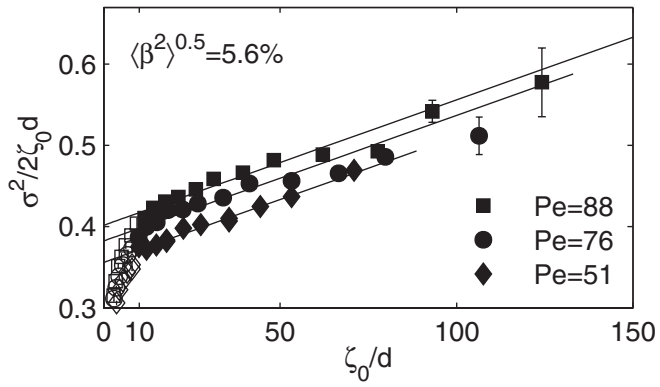

FIG. 2. Linear behavior of $\sigma^2/2\zeta_0 d$ vs ζ_0/d in the quasiasymptotic regime (III) fitted to expression (2), for pack $P3$.

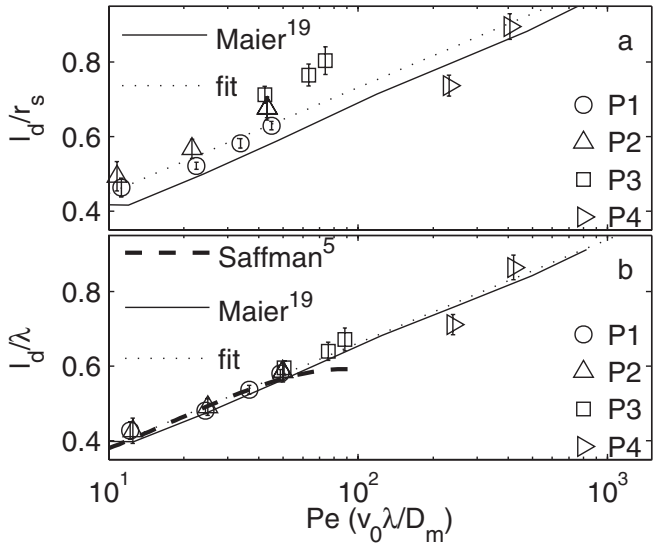

FIG. 3. (a) Dispersivities l_d scaled by respective sphere radii r_s, for our experiments and Maier's simulation. (b) Dispersivities l_d scaled by the respective hydrodynamic lengths $\lambda = 6r_h$, showing agreement of theory, simulation, and experiment. Dotted lines are fits to data.

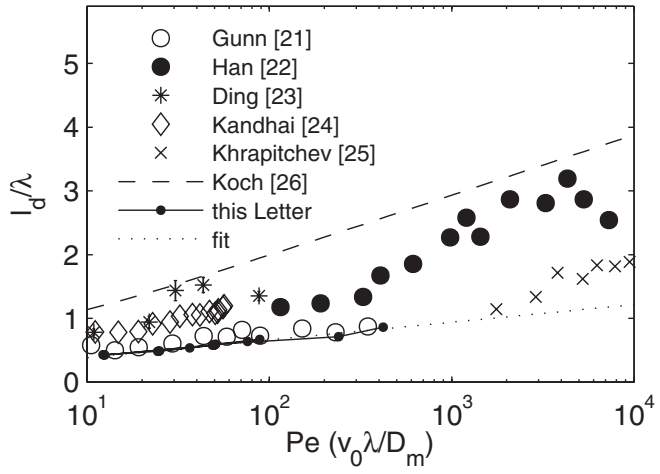

FIG. 4. Scaled experimental and theoretical dispersivities l_d/λ, from the literature.

remarkable coincidence indicates an intrinsic insensitivity of dispersion to details of the flow profile in a channel once the flow has been scrambled by mechanical mixing. While the ratio $\theta = l/a$ of the capillaries is determined by our measurement of dispersivity, the capillary radius a could be set by either matching the permeability of the capillary network $k_c = \varepsilon r_h^2/6$ [4] to experimentally determined permeabilities of packed spheres $k_s = \varepsilon r_h^2/C$, $C \approx 5.6 \pm 1$ [20], or by equating hydrodynamic radii of the pack and the network. Both approaches yield the same result, to within experimental error: $a = d \times 3/16$ and $l = d \times 0.72$, for $\varepsilon = 0.36$.

Figure 4 puts our results and extrapolated fit in the context of other workers' data obtained in regime (III), using either tracer [21,22] or NMR methods [23–25], assuming $\varepsilon = 0.37$ in the case of Ref. [23]. All results lie above ours and, according to our discussion above, should measure the true dispersivity plus an additive constant $\propto \langle \beta^2 \rangle$. This appears to be the case for the gas tracer experiments by Gunn and Pryce, which were obtained in the inertial to turbulent regime, with Reynolds numbers Re $\approx$ Pe for gas flow. The near coincidence of their turbulent results with our laminar results also indicates an insensitivity of dispersion to the flow profile at the pore scale, in the mechanically mixed regime. NMR results obtained at high Pe and $\zeta_0 = 10d$ [25] are less sensitive to macroscopic heterogeneities than the elution data [22] at the same Péclet number, and suggest either an upturn of dispersivity or provide an upper bound for l_d/λ. We also show Koch and Brady's result for dispersion by a rigid dilute suspension of monodisperse spheres which they extrapolated to denser packs with $\varepsilon = 0.5$ [26]. Their extrapolation set a lower bound for experimental data not shown here. The lack of agreement of extrapolated dilute results with all data in Fig. 4 becomes even more pronounced for lower porosities.

In conclusion, we have determined the intrinsic dispersivity of packed spheres with noninertial flows for Péclet numbers between 10 and 450. When scaled by the hydrodynamic radius our results, Saffman's prediction, and simulations for infinite packs collapse onto a single master curve with logarithmic dependence on Péclet number. The flow profile at the pore level, whether it is set by a straight pipe, by the curved channels in packed spheres, or by turbulence, does not appear to have pronounced effects on dispersivity in the mechanically mixed regime (III). Saffman's capillary model makes the correct quantitative link between dispersion and permeability, to within experimental error. Koch and Brady's extrapolation of results for the dilute limit fails for dense packs.

*ums@dq.fct.unl.pt

[1] G. I. Taylor, Proc. R. Soc. A **219**, 186 (1953).
[2] G. I. Taylor, Proc. R. Soc. A **225**, 473 (1954).
[3] R. Aris, Proc. R. Soc. A **235**, 67 (1956).
[4] P. G. Saffman, J. Fluid Mech. **6**, 321 (1959).
[5] P. G. Saffman, J. Fluid Mech. **7**, 194 (1960).
[6] H. D. Pfannkuch, Rev. Inst. Fr. Petrol. **18**, 215 (1963).
[7] M. Kaviany, *Principles of Heat Transfer in Porous Media* (Spinger-Verlag, New York, 1995), 2nd ed.
[8] S. Torquato, T. M. Truskett, and P. G. Debenedetti, Phys. Rev. Lett. **84**, 2064 (2000).
[9] D. Vortmeyer and J. Schuster, Chem. Eng. Sci. **38**, 1691 (1983).
[10] P. N. Pusey *et al.*, Phys. Rev. Lett. **63**, 2753 (1989).
[11] O. Pouliquen, M. Nicolas, and P. D. Weidman, Phys. Rev. Lett. **79**, 3640 (1997).
[12] R. M. Cotts *et al.*, J. Magn. Reson. **83**, 252 (1989).
[13] R. Kubo, M. Toda, and N. Hashitsume, *Statistical Physics II* (Springer-Verlag, Berlin, 1991).
[14] U. M. Scheven and P. N. Sen, Phys. Rev. Lett. **89**, 254501 (2002).
[15] U. M. Scheven *et al.*, Phys. Fluids **17**, 117107 (2005).
[16] L. Lebon *et al.*, Phys. Fluids **8**, 293 (1996).
[17] P. C. Carman, Trans. Inst. Chem. Eng. **15**, 150 (1937).
[18] R. S. Maier *et al.*, Phys. Fluids **15**, 3795 (2003).
[19] R. S. Maier *et al.*, Phys. Fluids **12**, 2065 (2000).
[20] A. P. Philipse and C. Pathmamanoharan, J. Colloid Interface Sci. **159**, 96 (1993).
[21] D. J. Gunn and C. Pryce, Trans. Inst. Chem. Eng. **47**, T341 (1969).
[22] N. W. Han, J. Bhakta, and R. G. Carbonell, AIChE J. **31**, 277 (1985).
[23] A. Ding and D. Candela, Phys. Rev. E **54**, 656 (1996).
[24] D. Kandhai *et al.*, Phys. Rev. Lett. **88**, 234501 (2002).
[25] A. A. Khrapitchev and P. T. Callaghan, Phys. Fluids **15**, 2649 (2003).
[26] D. Koch and J. F. Brady, J. Fluid Mech. **154**, 399 (1985).